Precision-targeted metabolomics method characterizes differential metabolomes in multiple-biological matrixes and cell-mitochondria

Xialin Luo[1, 2], Rui Guo[1, 2], Jingjing Liu[1, 2,], Aihua Zhang[3] Xijun Wang[3]* and Haitao Lu[1, 2]*

[1]Key Laboratory of Systems Biomedicine (Ministry of Education), Shanghai Center for Systems Biomedicine, Shanghai Jiao Tong University, Shanghai 200240, China

[2]Laboratory for Functional Metabolomics Science, Shanghai Jiao Tong University, Shanghai 200240, China

[3] National Chinmedomics Research Center, Sino-America Chinmedomics Technology Collaboration Center, National TCM Key Laboratory of Serum Pharmacochemistry, Heilongjiang University of Chinese Medicine, Heping Road 24, Harbin, 150040, China.

Corresponding authors

Haitao Lu., Ph.D., Professor, Shanghai Jiao Tong University

Email: haitao.lu@sjtu.edu.cn; Tel.: 86-15221478139

Xijun Wang., Ph.D., Professor, Heilongjiang University of Chinese Medicine

Email: xijunw@sina.com; Tel.: 86-13339512688

Abstract

Developing a precision LC-MS-based targeted metabolomics method for large-scale analysis of key metabolomes is likely to be of great value to investigations in the life sciences**.** Our new targeted-metabolomics method employs a reversed-phase liquid chromatography (RPLC) for non-polar metabolomes and hydrophilic interaction liquid chromatography (HILIC) for polar metabolomes with ultra-high performance liquid chromatography-triple-quadrupole mass spectrometry (UHPLC- TQ/MS) in a dynamic MRM scan-mode, we substantially increased the coverage to 240 metabolites of interest with largely variable polarity and improved detection capacity by fully optimizing analytical parameters with LC- and MS- units. This new method has the capacity to dynamically analyse the metabolome of interest in diverse biological matrixes by offering coverage of rat urine, plasma, liver, brain, intestine, stomach, heart, spleen, lung, faeces, fresh plant tissues, cells and microbes. In addition, this new method enables specific and efficient analysis of microdontia metabolomes, non-microdontia and whole cell metabolomes, as well as can engage in absolute determination of 84 key clinical-wide metabolites in different biological matrixes, to enable the complementary support of clinical diagnosis and classification of diseases. To demonstrate the applicable capacity of this new method, multiple-matrixes differential metabolomes were firstly characterized using this new method to coordinate metabolic modifications underlie hepatitis induced by carbon tetrachloride (CCL_4) in rats, such finding provides novel insight into the pathogenesis and therapeutics of hepatitis in clinic. Altogether, we are fully confident that this new

metabolomics method will be widely welcomed by scientists in different niches to solve their key questions accordingly.

Key Words: precision-targeted metabolomics, functional metabolomes, multiple biological-matrixes, mitochondria metabolism, biomarker discovery

Metabolism is characterized by a series of essential life-sustaining processes in all organisms through which living cells acquire necessary nutrients and energy, which enables cells to grow, differentiate and function. By characterizing the altered metabolism underlying diverse biochemical events and/or processes, we could solve key problems in different niches, such as biomedicine, bioengineering, agriculture and the environment[1-3]. In the late 1990s, a systems biology-driven metabolomics method was first proposed to provide a comprehensive approach to precisely investigate metabolism[4,5] via global and quantitative analyses of endogenous metabolites in biological systems that require data acquired through high-resolution analytical technologies[6].

To the best of our knowledge, untargeted metabolomics is seriously limited to the identification of differential metabolites for which reference compounds are unavailable and often provides only the metabolic phenotypes[7,8], such that no functional experiments can be completed without the purified compounds of interest. In contrast, obtaining reference compounds is facilitated by targeted metabolomics and is becoming a prevalent methodology for studying functional metabolism, owing to the commercial availability of the differential compounds, and further functional studies on regulatory genes and biosynthetic enzymes can help precisely determine the biochemical mechanisms underlies the altered metabolism[9,10]. Developing a high-throughput LC-MS-based targeted metabolomics method for large-scale analysis of known metabolomes is likely to be of great value to investigations in the life sciences[11,12, 13].

With this new-developed metabolomics method, referring to our prior publication in JPR in 2011[13], we were the first to optimally select and retrieve 240 small-molecule metabolites with important biological functions featured broadly in key publications **(Figure 1),** including organic acids, fatty acids, sugars, phosphate-sugars, amino acids and lipids, that are closely associated with disease progression, pathogenesis and therapeutic discovery[13-16]. Then, UHPLC-TQ/MS parameters was fully optimized to enable reversed-phase liquid chromatography (RPLC) for non-polar metabolomes assay and hydrophilic interaction liquid chromatography (HILIC) for polar metabolomes assay **(Figure 2)** in a dynamic MRM scan-mode **(Table S1).** This new method has the capacity to significantly enhance the detectable levels of the metabolites of interest and widens the coverage to include their polarity [17-18] **(Figure 3).**

To tailor the translational applicability of this method for use in the full-spectrum of life sciences, we sought to analyse the metabolomes of interest present in a range of diverse biological matrixes **(Figure 4).** It is exciting to illustrate the collective data that this protocol has been able to obtain efficiently for targeted characterization of metabolomes from rat urine, plasma, liver, brain, intestine, stomach, heart, spleen, lung and faeces; fresh plant tissues; cells; and microbes **(Figure 5A and C).** Importantly, in terms of microdontia, it is quite important to understand the related cell metabolism, because metabolic dysregulation is implicated in numerous important biological processes and events, such as cancers, diabetes, and immunological deficiency, and the whole cell-metabolome assay often cannot be used

for precise characterization of the functional features of dysregulated microdontia related to different biological events. To improve this assay, our new protocol was developed to enable the simultaneous analysis of microdontia metabolomes, non-microdontia metabolomes, and whole-cell metabolomes **(Figure 5B)**. When making a comparison among cancer cell lines, microdontia metabolomes are much better than non-microdontia metabolomes or whole-cell metabolomes for investigating metabolic reprogramming during cancer progression. Finally, for improved clinical diagnosis and classification of targeted diseases, we also determined calibration curves for precise quantification of metabolite biomarkers, and 84 key metabolites were eventually and absolutely quantified in both plasma and urine samples, as well as other tissue matrixes **(Tables 2 and 3).** Collectively, the rapid determination of these 84 key metabolites with our targeted metabolomics protocol has great potential for use in complementing the clinical diagnosis of complex diseases **(Figure 6)**. To demonstrate the applicable capacity of this new method, multiple-matrixes differential metabolomes were firstly characterized using this new method to coordinate metabolic modifications underlie hepatitis induced by carbon tetrachloride (CCL_4) in rats. Such findings verify the robustness and applicable potential of this new targeted metabolomics method, as well as provide novel insight into the pathogenesis and therapeutics of hepatitis in clinic from multisensorial metabolic perspective **(Figure 7).**

Taking all these advantages together, this novel protocol for targeted metabolome assays has substantial coverage of 240 key metabolites in dozens of important

metabolic pathways. This method can enable the use of metabolome assays with different biological matrixes and offers a new horizon for analyses of microdontia metabolomes, non-microdontia metabolomes, and whole-cell metabolomes.

In short, this new method is far better than previous protocols of targeted metabolome assays, particularly in terms of matrix adaptation, capacity for absolute quantification, and new and future applications for the analysis of microdontia metabolomes and non-microdontia metabolomes. We are fully confident that this protocol will be widely welcomed by scientists studying different biological niches to solve their key questions accordingly **(Figure 8).**

Materials and Methods

Chemicals and reagents

All of reference compounds for targeted metabolomes of interest (**Table 1**) were purchased from Sigma-Aldrich Corp (Saint Louis, USA), and 1 mg/mL stock solution was prepared by dissolving them into water or methanol, respectively. Methanol, acetonitrile and formic acid (HPLC-grade) were purchased from Thermo Fisher Scientific (Shanghai, China). Ammonium acetate (HPLC grade) was purchased from Merck KGaA (Darmstadt, Germany). LB broth (Luria−Bertani) and LB agar were purchased from Becton Dickinson (Sparks, USA). Magnesium sulfate, manganese chloride, casamino acid, yeast extract, of USP grade, were purchased from Sigma-Aldrich Corp (Saint Louis, USA). The distilled water was purchased from A.S. Watson Group (Guangzhou, China). All other reagents were of ACS grade.

UPLC/TQ MS system

An UPLC system (1290 Infinity series, Agilent Technologies) coupled to a triple quadrupole mass spectrometer (Agilent 6495, Agilent Technologies) was used for precision-targeted metabolome assay in a dynamic MRM mode (DMRM). The optimized dynamic MRM parameters for the targeted metabolomes were listed in **Table 1**. The key parameters for MS unit are briefly summarized as, the ion source was Agilent Jet Stream ESI and the parameters were set as follows: dry gas temperature, 250 ^{o}C; dry gas flow, 16 L/min; nebulizer pressure, 20 psi; sheath gas heater, 350 ^{o}C; sheath gas flow, 12 L/min; capillary voltage, capillary voltage, 4000 V for positive mode and 3500 V for negative mode. RPLC separation was performed with an ACQUITY UPLC HSS T3 (2.1×100 mm, 1.8 μm) column; the mobile phase A was water with 0.1% formic acid (v/v) and mobile phase B was acetonitrile with 0.1% formic acid (v/v) with an optimized gradient-elution program: 0-2 min, 98% A; 2-10 min, 98%-65% A; 10-12 min, 65%-20% A; 12-14 min, 20%-2% A; 14-30 min, 2% A. HILIC separation was carried out with an ACQUITY UPLC BEH Amide column (2.1 mm i.d×100 mm, 1.7 μm; Waters), the mobile phase A is changed to water with 0.1% (v/v) formic acid and 10mM ammonium acetate, while mobile phase B is acetonitrile with 0.1% formic acid (v/v); the relevant gradient-elution program was optimized as: 0-4 min, 5% -12% A; 4-15min, 12%-50%; 15-25 min, 50% A. The flow rate for both RPLC and HILIC separation systems was set at 0.3 mL/min and the column temperature was maintained at 40 ^{o}C. All the samples were placed in 10 °C with a 5 μL-volume injection.

Rat sampling and collection

Male SD rats (age: 6 weeks, body weight: 160-200 g) were supplied by GLP Center of Heilongjiang University of Chinese Medicine (Harbin, China). In treated group, 6 rats were orally intraperitoneal injected with 20% CCl_4 olive oil solution according to the rat weight at 5 mL/kg, to induce liver injury, another 6 rats were treated with olive oil solution as healthy controls. Urinary samples were collected with metabolic-cage and centrifuged under 13000 rpm at 4 °C for 15 min. The rats were sacrificed by exsanguination after anesthetized by intraperitoneal injection of 3% pentobarbital sodium according to the rat weight at 2 mL/kg, and the plasma samples were collected and centrifuged under 3500 rpm at 4 °C for 15 min. In addition, the tissues, such as brain, heart, liver, spleen, kidney, small intestine, and lung samples were collected and cleaned in normal saline, then rapidly frozen in liquid nitrogen. Finally, tissues, urine and plasma samples were all stored at -80 °C until use. All animal care and experimental procedures were performed in compliance with the rules on the care and use of animals of the Ethical Committee of Heilongjiang University of Chinese Medicine. All efforts were made to ameliorate the suffering of the animals.

Bacterial strains and cultivation

The UTI89 and MG1655 strains were firstly cultured in LB-agar plate for 12 h, then one colony was collected to incubated with LB broth medium for 4 h, diluted 1000-fold into CFA medium and further cultivated for 72 h at 30°C to trigger mature

biofilm formation. CFA medium is consisted of 1% Casamino acids, 0.15% yeast extract, 0.005% magnesium sulfate and 0.0005% manganese chloride.

Isolation of mitochondria from cells

Cell line Panc-1 was purchased from the American Type Culture Collection (ATCC) , the cells are cultured in DMEM medium supplied with 10% fetal bovine serum and 1% Penicillin-Streptomycin, maintained at 37°C in a humidified atmosphere containing 5% CO_2. In order to obtain a significant quantity of mitochondria, an appropriate number at about 3 million cells were seeded in a 150 mm dish and grown to approximately 2×10^7 cells. The isolated mitochondria and cytosolic fraction were achieved by commercially available mitochondria isolation kit (Beyotime, China). The isolation was performed according to a modified manufacturer's protocol. Briefly, cells were washed with ice cold PBS, followed by adding 1 mL of the prepared 1×Extraction Buffer A, then incubated on ice for 10 minutes. To further homogenize the cells on ice with a dounce homogenizer for 15 strokes. The extraction was centrifuged under 600 × g for 10 minutes at 4 °C, and carefully transfer the supernatant into a new PE tube, centrifuge under 11,000 × g for 10 minutes at 4 °C. At last, the supernatant was collected as cytosolic fraction and the pellets were mitochondria. All the isolation process should be performed on ice.

Metabolome extraction

Body fluids Referring to our previous protocol[13], we made a revised version as below,

briefly, the urine samples could be directly analyzed with LC-TQ MS after a simple preparation as urinary samples were centrifuged under 20,000 g at 4 ^{o}C for 10 min and filtered by 0.22 μm Millipore filter. 100 uL of plasma samples were mixed with 4 volume of iced-cold acetonitrile to precipitate proteins, then centrifuged to 20,000 g for 10 min at 4 ^{o}C. Following the supernatant was transferred to a new 1.5-mL microcentrifuge tube and dried with N_2, finally dissolved in 100 μl of water and centrifuged again before analyzed by LC-TQ MS.

Tissues Brain, heart, liver, spleen, kidney, small intestine and lung share the same protocol for metabolome extraction. About 100-130 mg tissue samples were weighed and placed into a 2-mL screw-cap plastic microvials containing about 1 g glass beads (1.0 mm i.d.). Then tissues were completely homogenized at a 2-min run for 3 times (after one run we need to put the sample on ice for cooling) in 1.2 ml of 80% ice-cold methanol by Mini-Beadbeater-16 (Biospec Products). After that, spun down at 20,000 g for 10 min and vortexed with 800 μl of iced-cold acetonitrile, centrifuged again to remove the protein precipitates. The supernatant was processed following the same procedure as plasma samples. Quality control (QC) samples by pooling aliquots of all samples were analyzed during the whole LC-TQ MS analysis.

Bacterial strains Referring to the previous protocol[14], we made a revised version. Firstly, biofilm samples were isolated from 50 mL of culture solution, to obtain the planktonic cells, the supernatants in the culture medium were centrifuged to 931 g at 4

^{o}C for 15 min. After wash the biofilm with 2 mL PBS for 3 times, add 2 mL of 80% ice-cold methanol, homogenize by homogenizer for 2 minutes, 3 times. All procedures were performed on ice for cooling. Then, the homogenate was spun down at 13201 g to collect the supernatants. After adding 800 μL of ice-cold acetonitrile, centrifuged again, the fresh supernatants were filtered through 0.22μm filter membrane and stored in -80℃before lyophilization. The lyophilized samples were dissolved in 100 μL of water and centrifuged again before analyzed with LC-TQ MS.

Cells, cytoplasm and mitochondrial metabolome extraction of the isolated mitochondrial was done by following the same procedure as that of tissue samples except for replacing the 1.0 mm i.d. of glass beads with 0.5 mm. The cytoplasm samples were mixed with 800 μL iced-cold acetonitrile to precipitate proteins, then following the steps of plasma-metabolome preparation. For whole cells, firstly, wash cells twice with PBS, following add 1.2 mL 80% ice cold aqueous methanol and all the cells were harvested by cell scraper on ice, and transferred to a 2-mL screw-cap plastic micro-vial, then homogenized, centrifuged; at last, adding iced-cold acetonitrile and following the routine procedure as the metabolome extraction of bacterial cells.

Absolute determination of key clinical-wide metabolites

To assist clinical diagnosis of a variety of diseases with this new developed metabolomics method, we adopted a set of external standards by containing at least

five-levels concentration to establish the calibration curve. 84 key clinical-wide metabolites can be absolutely determined by the developed precision-targeted metabolomics method **(Table S2)**. In this case, we attempt to verify the efficiency of this new developed method by selectively determining the absolute concentration of 27 key metabolites present in a diverse biological-matrixes **(Table S3)**.

Data Processing and Statistical Analysis

The MS raw data generated from the biological samples was firstly processed by qualitative Analysis, with an in-house software of Agilent Corps, which integrated the signal-peaks and generated a three-dimension data-matrixes with peak-area of merabolite-metabolite ID-sample ID. After peak area for each metabolite was normalized to tissue weight of each sample, the processed data was uploaded onto free MetaboAnalyst online-softare (http://www.metaboanalyst.ca/MetaboAnalyst/) for partial least-squares discriminant analysis (PLS-DA) and heatmap vs hierarchical-cluster analysis (HCA).

Acknowledgements

This work was supported by the National Key R&D Program of China (No. 2017YFC1308600 and 2017YFC1308605), the National Natural Science Foundation of China Grants (No. 81274175 and 31670031), the Startup Funding for Specialized Professorship Provided by Shanghai Jiao Tong University (No. WF220441502), and the Fundamental Research Funds for the Central Universities (grant no.

106112015CDJZR468808).

References

1 Jang, C., Chen, L. & Rabinowitz, J. D. Metabolomics and Isotope Tracing. *Cell* **173**, 822-837, doi:10.1016/j.cell.2018.03.055 (2018).

2 Boulange, C. L., Neves, A. L., Chilloux, J., Nicholson, J. K. & Dumas, M. E. Impact of the gut microbiota on inflammation, obesity, and metabolic disease. *Genome Med* **8**, 42, doi:10.1186/s13073-016-0303-2 (2016).

3 Geiger, R. *et al.* L-Arginine Modulates T Cell Metabolism and Enhances Survival and Anti-tumor Activity. *Cell* **167**, 829-842.e813, doi:10.1016/j.cell.2016.09.031 (2016).

4 Oliver, S. G., Winson, M. K., Kell, D. B. & Baganz, F. Systematic functional analysis of the yeast genome. *Trends Biotechnol* **16**, 373-378, doi:Doi 10.1016/S0167-7799(98)01214-1 (1998).

5 Nicholson, J. K., Lindon, J. C. & Holmes, E. 'Metabonomics': understanding the metabolic responses of living systems to pathophysiological stimuli via multivariate statistical analysis of biological NMR spectroscopic data. *Xenobiotica* **29**, 1181-1189, doi:Doi 10.1080/004982599238047 (1999).

6 Winder, C. L., Dunn, W. B. & Goodacre, R. TARDIS-based microbial metabolomics: time and relative differences in systems. *Trends Microbiol* **19**, 315-322, doi:10.1016/j.tim.2011.05.004 (2011).

7 Want, E. J. *et al.* Global metabolic profiling of animal and human tissues via UPLC-MS. *Nature protocols* **8**, 17-32, doi:10.1038/nprot.2012.135 (2013).

8 Want, E. J. *et al*. Global metabolic profiling procedures for urine using UPLC-MS. *Nature protocols* **5**, 1005-1018, doi:10.1038/nprot.2010.50 (2010).

9 Kuo, M. T., Savaraj, N. & Feun, L. G. Targeted cellular metabolism for cancer chemotherapy with recombinant arginine-degrading enzymes. *Oncotarget* **1**, 246-251, doi:10.18632/oncotarget.135 (2010).

10 Luo, X. *et al*. Mass spectrometry and associated technologies delineate the advantageously biomedical capacity of siderophores in different pathogenic contexts. *Mass Spectrometry Reviews* **0**, doi:doi:10.1002/mas.21577.

11 Cai, Y., Weng, K., Guo, Y., Peng, J. & Zhu, Z.-J. An integrated targeted metabolomic platform for high-throughput metabolite profiling and automated data processing. *Metabolomics* **11**, 1575-1586, doi:10.1007/s11306-015-0809-4 (2015).

12 Wei, R., Li, G. D. & Seymour, A. B. High-Throughput and Multiplexed LC/MS/MRM Method for Targeted Metabolomics. *Analytical chemistry* **82**, 5527-5533, doi:10.1021/ac100331b (2010).

13 Lv, H., Palacios, G., Hartil, K. & Kurland, I. J. Advantages of tandem LC-MS for the rapid assessment of tissue-specific metabolic complexity using a pentafluorophenylpropyl stationary phase. *Journal of proteome research* **10**, 2104-2112, doi:10.1021/pr1011119 (2011).

14 Su, Q., Guan, T., He, Y. & Lv, H. Siderophore Biosynthesis Governs the Virulence of Uropathogenic Escherichia coli by Coordinately Modulating the Differential Metabolism. *Journal of proteome research* **15**, 1323-1332, doi:10.1021/acs.jproteome.6b00061 (2016).

15 Lv, H., Hung, C. S., Chaturvedi, K. S., Hooton, T. M. & Henderson, J. P. Development of an integrated metabolomic profiling approach for infectious diseases research. *Analyst* **136**, 4752-4763, doi:10.1039/c1an15590c (2011).

16 Lv, H. *et al.* Ingenuity pathways analysis of urine metabonomics phenotypes toxicity of gentamicin in multiple organs. *Mol Biosyst* **6**, 2056-2067, doi:10.1039/c0mb00064g (2010).

17 Domingo-Almenara, X. *et al.* XCMS-MRM and METLIN-MRM: a cloud library and public resource for targeted analysis of small molecules. *Nat Methods* **15**, 681-684, doi:10.1038/s41592-018-0110-3 (2018).

18 Rao, Z. *et al.* Development of a dynamic multiple reaction monitoring method for determination of digoxin and six active components of Ginkgo biloba leaf extract in rat plasma. *Journal of chromatography. B, Analytical technologies in the biomedical and life sciences* **959**, 27-35, doi:10.1016/j.jchromb.2014.03.028 (2014).

Figure Legends

Figure 1. 240 key metabolites with importantly biochemical functions are captured by the proposed targeted metabolomics method.

Figure 2. schematic illustration of the developed targeted-metabolomics method from the optimization of analytical parameters, high-quality data-acquisition, data analysis/visualization, absolute determination of key metabolites to the capacity of enabling translational applications in different niches of life sciences.

Figure 3. Typical reference-compound EIC profiles for 240 targeted metabolites collected by both by reverse-phase T3 column (A, B and C), and normal-phase HILIC column (D).

Figure 3. schematic illustration of the developed targeted-metabolomics method from the optimization of analytical parameters, high-quality data-acquisition, data analysis/visualization, absolute determination of key metabolites to the capacity of enabling translational applications in different niches of life sciences.

Figure 4. Heatmap overview of differential metabolomes with selected tissues

Figure 5. The targeted metabolomics method can be broadly used for precision-assay

of differential metabolomes in differently biological-matrixes, including tissues, biological fluids and feces (A); mitochondria, cytoplasm and whole cells (B); and microbial organisms (C).

Figure 6. 84 clinical-wide key metabolites can be absolutely determined from different biological matrixes with our new targeted-metabolomics method, particularly urine and plasm. Such effort can complementarily support clinical diagnosis of numerous diseases.

Figure 7. this method is used to characterize metabolic pattern throughout multiple tissues of hepatitis induced by CCL_4 in rats. The data completely reveals high-resolution metabolic modifications of hepatitis that are closely associated with different tissues besides liver. Such findings verify the robustness and applicable potential of this new targeted metabolomics method, as well as provide novel insights into unpredictable metabolic features of hepatitis to enable future pathogenesis annotation and therapeutic discovery.

Figure 8. Unique features of this new targeted metabolomics method are highlighted as 1) using an RPLC column for a hydrophilic metabolome assay and a HILIC column for a hydrophobic metabolome assay. 2) with our new targeted metabolomics protocol, we substantially increased the coverage to 240 metabolites of interest with largely variable polarity and improved detection capacity. 3) this new protocol has the

capacity to dynamically analyse the metabolome of interest in diverse biological matrixes by offering coverage of rat urine, plasma, liver, brain, intestine, stomach, heart, spleen, lung and faeces; fresh plant tissues; cells; and microbes. 4) this protocol enables specific and efficient analysis of microdontia metabolomes, non-microdontia and whole cell metabolomes. 5) absolute determination of 84 key metabolites in different biological matrixes enables the complementary support of clinical diagnosis and classification of diseases.

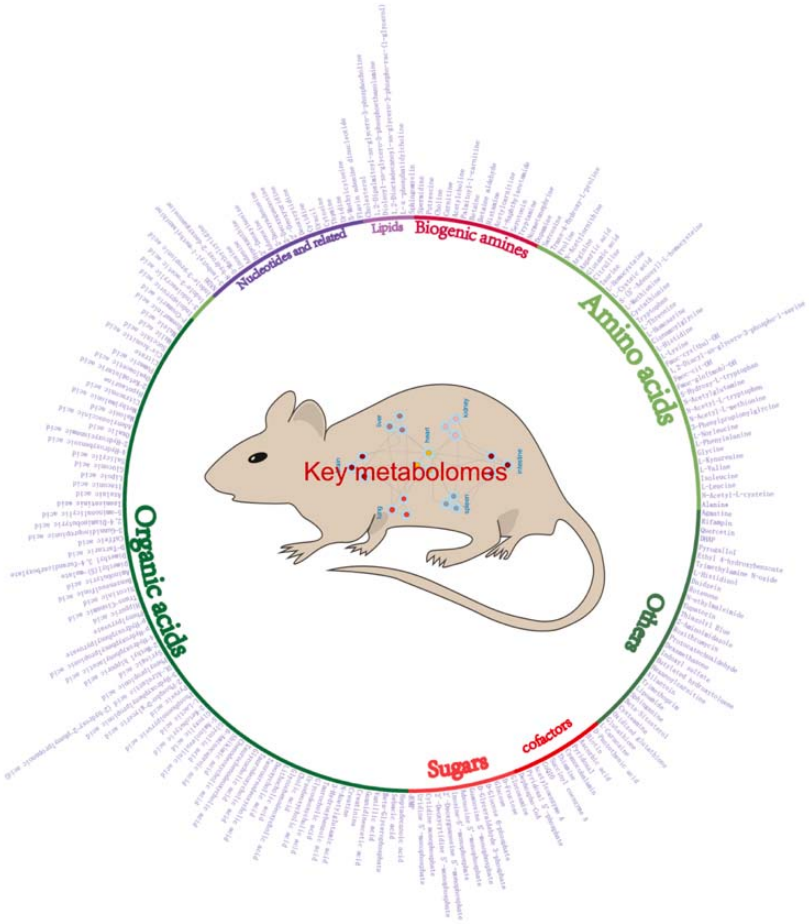
Nucleotides and related
Lipids
Biogenic amines
Amino acids
Others
cofactors
Sugars
Organic acids
Key metabolomes

Figure 1

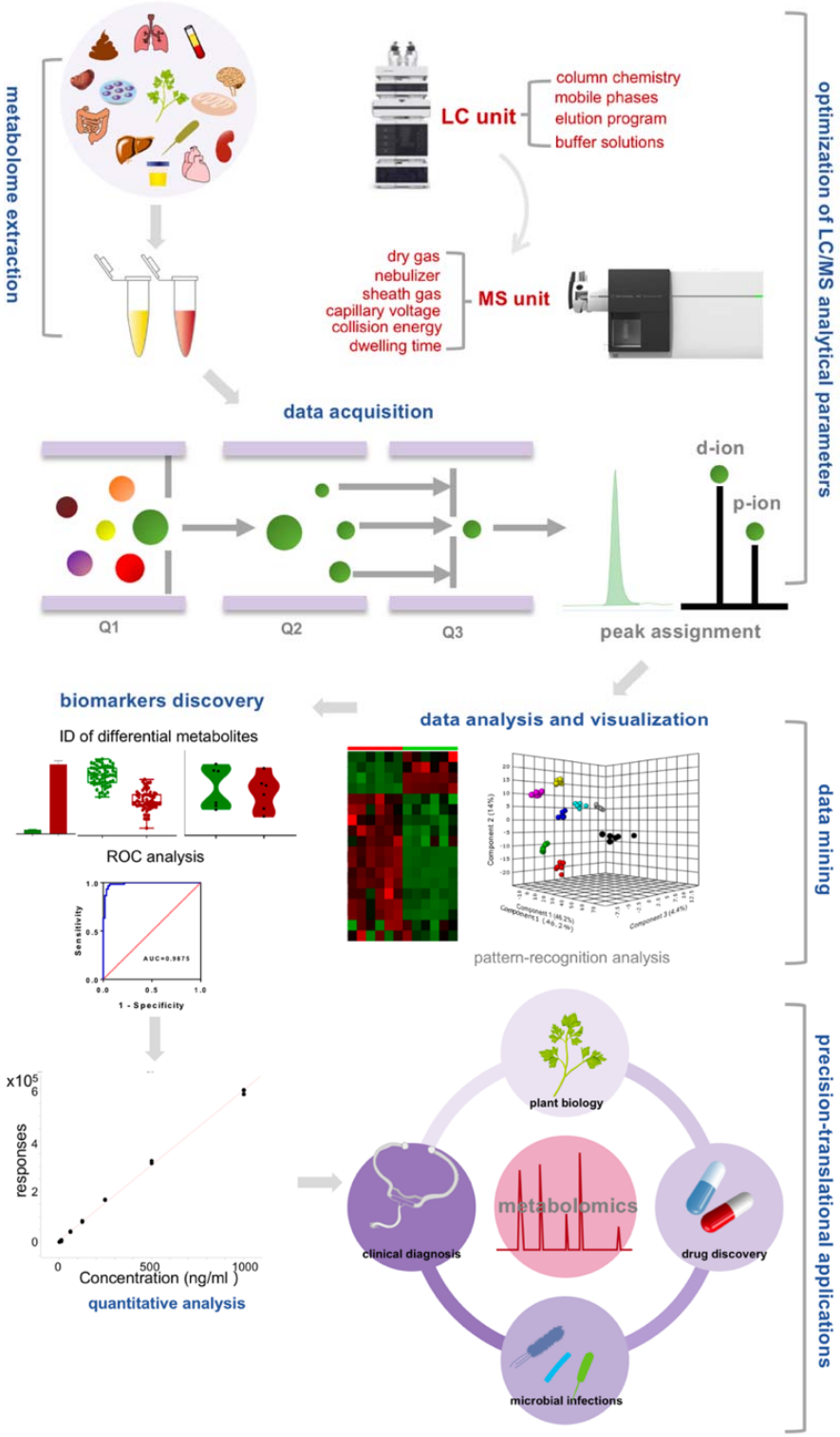
metabolome extraction
LC unit
column chemistry
mobile phases
elution program
buffer solutions
MS unit
dry gas
nebulizer
sheath gas
capillary voltage
collision energy
dwelling time
optimization of LC/MS analytical parameters
data acquisition
Q1
Q2
Q3
d-ion
p-ion
peak assignment
biomarkers discovery
ID of differential metabolites
ROC analysis
data analysis and visualization
pattern-recognition analysis
data mining
responses
Concentration (ng/ml)
quantitative analysis
plant biology
clinical diagnosis
metabolomics
drug discovery
microbial infections
precision-translational applications

Figure 2

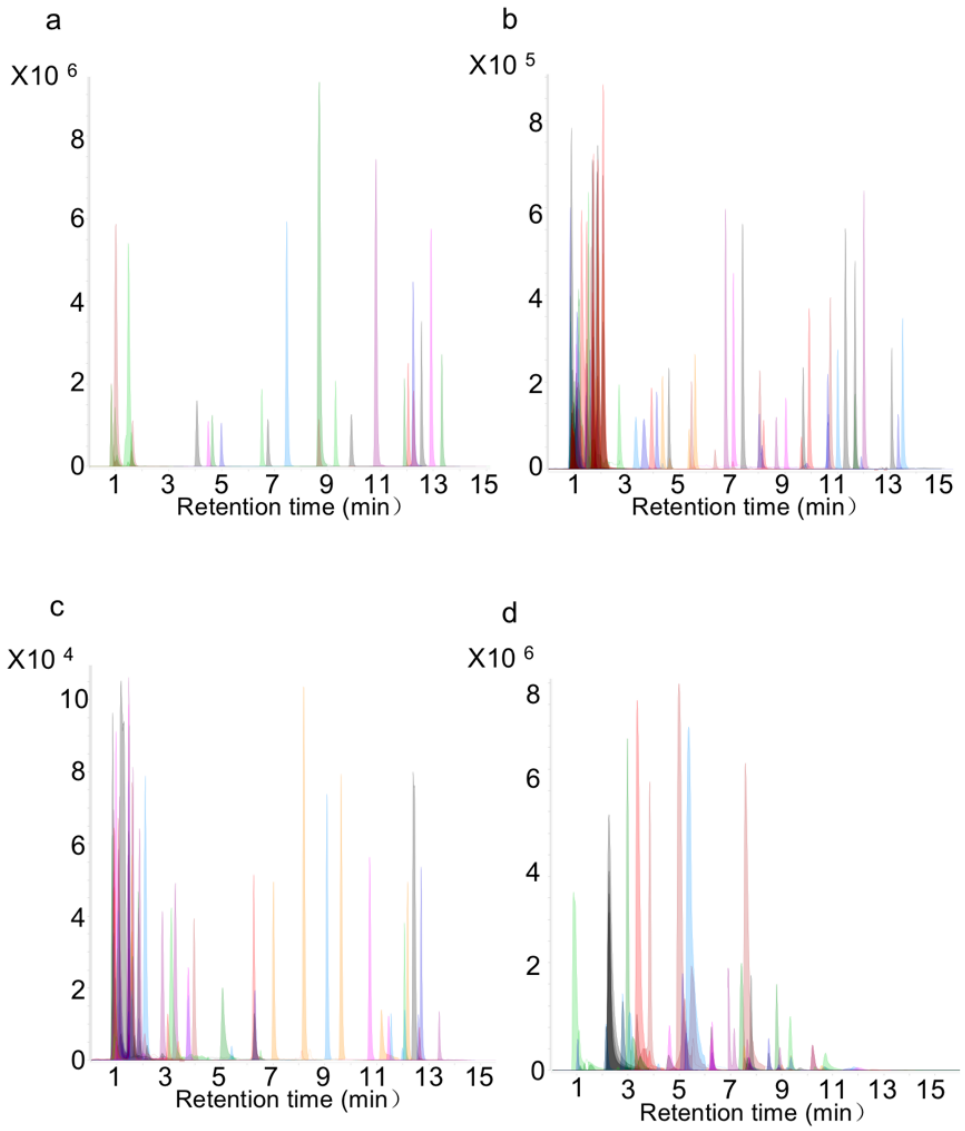
a
X10 6
8
6
4
2
0
1 3 5 7 9 11 13 15
Retention time (min)
b
X10 5
8
6
4
2
0
1 3 5 7 9 11 13 15
Retention time (min)
c
X10 4
10
8
6
4
2
0
1 3 5 7 9 11 13 15
Retention time (min)
d
X10 6
8
6
4
2
0
1 3 5 7 9 11 13 15
Retention time (min)

Figure 3

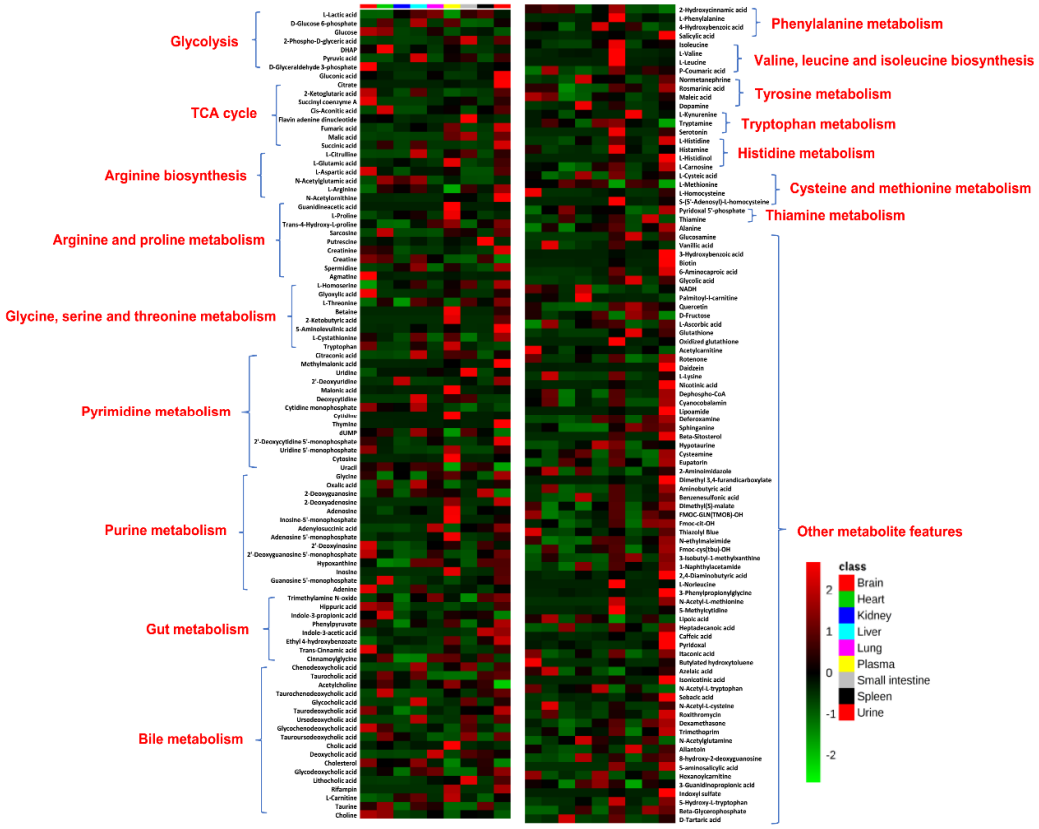
Glycolysis
L-Lactic acid
D-Glucose 6-phosphate
Glucose
2-Phospho-D-glyceric acid
DHAP
Pyruvic acid
D-Glyceraldehyde 3-phosphate
Gluconic acid
TCA cycle
Citrate
2-Ketoglutaric acid
Succinyl coenzyme A
Cis-Aconitic acid
Flavin adenine dinucleotide
Fumaric acid
Malic acid
Succinic acid
Arginine biosynthesis
L-Citrulline
L-Glutamic acid
L-Aspartic acid
N-Acetylglutamic acid
L-Arginine
N-Acetylornithine
Arginine and proline metabolism
Guanidineacetic acid
L-Proline
Trans-4-Hydroxy-L-proline
Sarcosine
Putrescine
Creatinine
Creatine
Spermidine
Agmatine
Glycine, serine and threonine metabolism
L-Homoserine
Glyoxylic acid
L-Threonine
Betaine
2-Ketobutyric acid
5-Aminolevulinic acid
L-Cystathionine
Tryptophan
Pyrimidine metabolism
Citraconic acid
Methylmalonic acid
Uridine
2'-Deoxyuridine
Maleinic acid
Deoxycytidine
Cytidine monophosphate
Cytosine
Thymine
dUMP
2'-Deoxycytidine 5'-monophosphate
Uridine 5' monophosphate
Cytosine
Uracil
Purine metabolism
Glycine
Oxalic acid
2-Deoxyguanosine
2-Deoxyadenosine
Adenosine
Inosine-5'-monophosphate
Adenylosuccinic acid
Adenosine 5'-monophosphate
2'-Deoxyinosine
2'-Deoxyguanosine 5'-monophosphate
Hypoxanthine
Inosine
Guanosine 5'-monophosphate
Adenine
Gut metabolism
Trimethylamine N-oxide
Hippuric acid
Indole-3-propionic acid
Phenylpyruvate
Indole-3-acetic acid
Ethyl 4-hydroxybenzoate
Trans-Cinnamic acid
Cinnamoylglycine
Bile metabolism
Chenodeoxycholic acid
Taurocholic acid
Acetylcholine
Taurochenodeoxycholic acid
Glycocholic acid
Taurodeoxycholic acid
Ursodeoxycholic acid
Glycochenodeoxycholic acid
Tauroursodeoxycholic acid
Cholic acid
Deoxycholic acid
Cholesterol
Glycodeoxycholic acid
Lithocholic acid
Rifampin
L-Carnitine
Taurine
Choline
Phenylalanine metabolism
2-Hydroxycinnamic acid
L-Phenylalanine
4-Hydroxybenzoic acid
Salicylic acid
Valine, leucine and isoleucine biosynthesis
Isoleucine
L-Valine
L-Leucine
P-Coumaric acid
Tyrosine metabolism
Normetanephrine
Rosmarinic acid
Maleic acid
Dopamine
L-Kynurenine
Tryptophan metabolism
Tryptamine
Serotonin
Histidine metabolism
L-Histidine
Histamine
L-Histidinol
L-Carnosine
Cysteine and methionine metabolism
L-Cysteic acid
L-Methionine
L-Homocysteine
S-(5'-Adenosyl)-L-homocysteine
Thiamine metabolism
Pyridoxal 5'-phosphate
Thiamine
Other metabolite features
Alanine
Glucosamine
Vanillic acid
3-Hydroxybenzoic acid
Biotin
6-Aminocaproic acid
Glycolic acid
NADH
Palmitoyl-L-carnitine
Quercetin
D-Fructose
L-Ascorbic acid
Glutathione
Oxidized glutathione
Acetylcarnitine
Rotenone
Daidzein
L-Lysine
Nicotinic acid
Dephospho-CoA
Cyanocobalamin
Lipoamide
Deferoxamine
Sphinganine
Beta-Sitosterol
Hypotaurine
Cysteamine
Eupatorin
2-Aminoimidazole
Dimethyl 5,4-furandicarboxylate
Aminobutyric acid
Benzenesulfonic acid
Dimethyl(S)-malate
FMOC-GLN(TMOB)-OH
Fmoc-cit-OH
Thioacetyl Blue
N-ethylmaleimide
Fmoc-cys(tbu)-OH
3-Isobutyl-1-methylxanthine
1-Naphthylacetamide
2,4-Diaminobutyric acid
L-Norleucine
3-Phenylpropionylglycine
N-Acetyl-L-methionine
5-Methylcytidine
Lipoic acid
Heptadecanoic acid
Caffeic acid
Pyridoxal
Itaconic acid
Butylated hydroxytoluene
Azelaic acid
Isonicotinic acid
N-Acetyl-L-tryptophan
Sebacic acid
N-Acetyl-L-cysteine
Roxithromycin
Dexamethasone
Trimethoprim
N-Acetylglutamine
Allantoin
8-hydroxy-2-deoxyguanosine
5-aminosalicylic acid
Hexanoylcarnitine
3-Guanidinopropionic acid
Indoxyl sulfate
5-Hydroxy-L-tryptophan
Beta-Glycerophosphate
D-Tartaric acid
2
1
0
-1
-2
class
Brain
Heart
Kidney
Liver
Lung
Plasma
Small intestine
Spleen
Urine

Figure 4

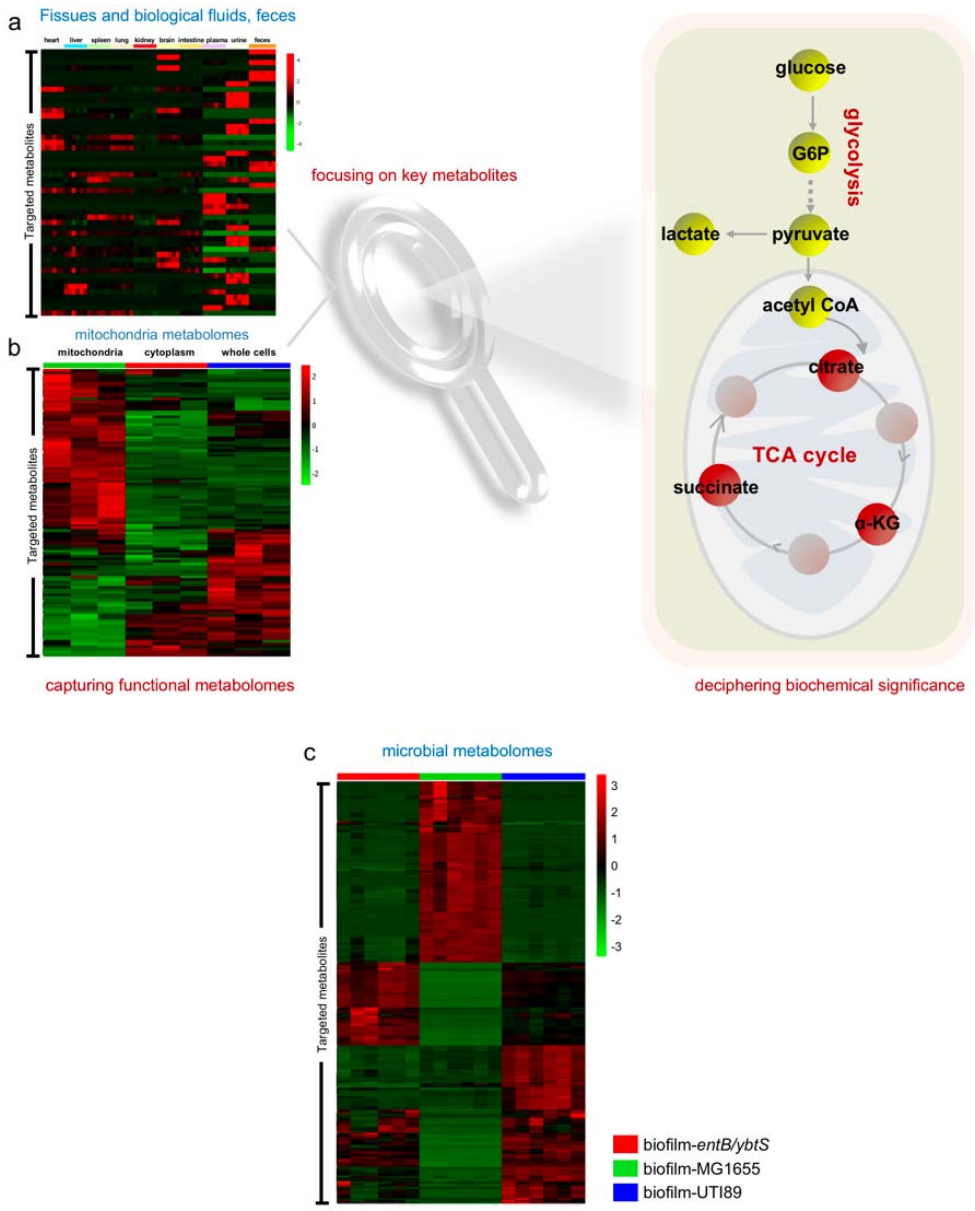
a
Fissues and biological fluids, feces
heart
liver
spleen
lung
kidney
brain
intestine
plasma
urine
feces
Targeted metabolites
focusing on key metabolites
b
mitochondria metabolomes
mitochondria
cytoplasm
whole cells
Targeted metabolites
capturing functional metabolomes
glucose
G6P
glycolysis
lactate
pyruvate
acetyl CoA
citrate
TCA cycle
succinate
α-KG
deciphering biochemical significance
c
microbial metabolomes
Targeted metabolites
biofilm-entB/ybtS
biofilm-MG1655
biofilm-UTI89

Figure 5

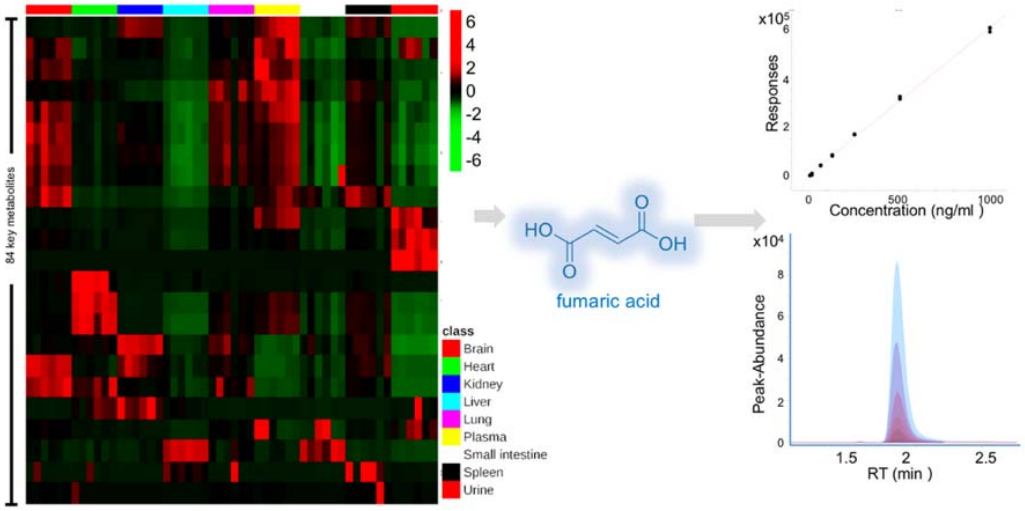
84 key metabolites
6
4
2
0
-2
-4
-6
class
Brain
Heart
Kidney
Liver
Lung
Plasma
Small intestine
Spleen
Urine
HO
O
O
OH
fumaric acid
x10^5
Responses
Concentration (ng/ml)
x10^4
Peak-Abundance
RT (min)

Figure 6

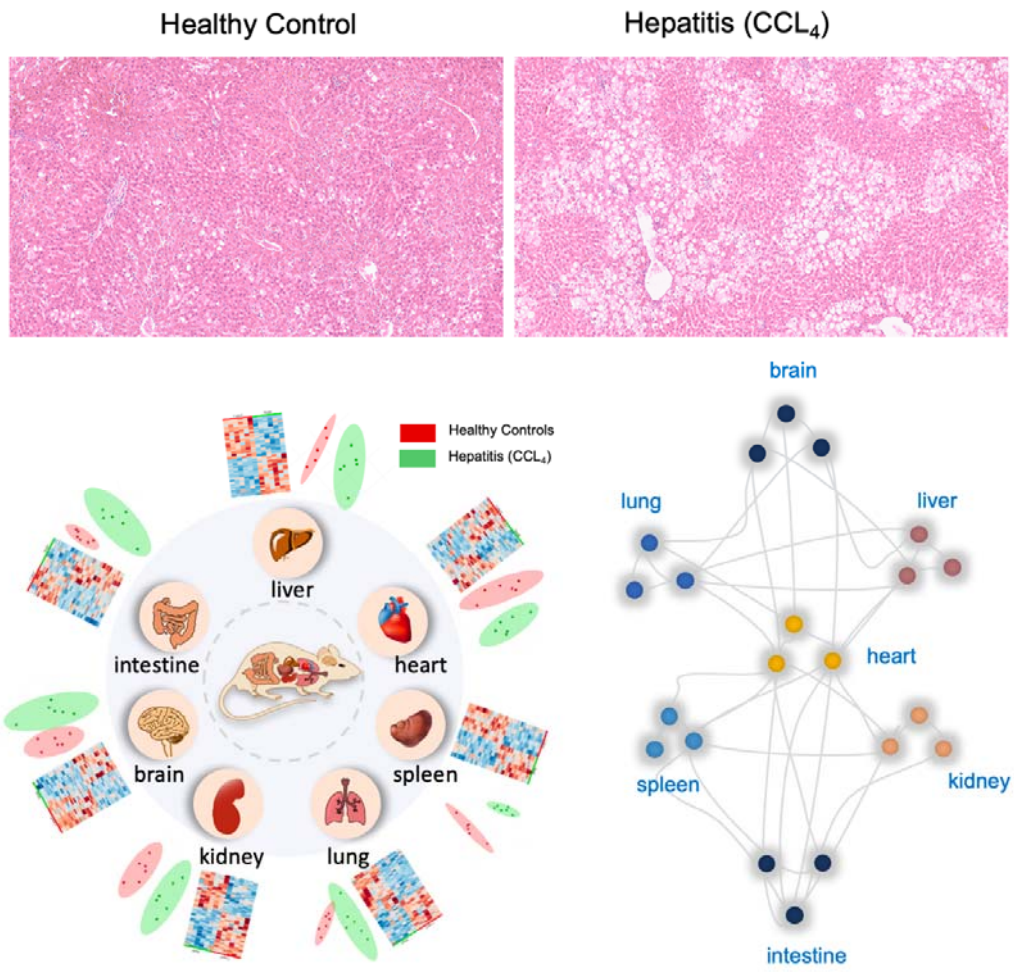
Healthy Control
Hepatitis (CCL_4)
Healthy Controls
Hepatitis (CCL_4)
liver
intestine
heart
brain
spleen
kidney
lung
brain
lung
liver
heart
spleen
kidney
intestine

Figure 7

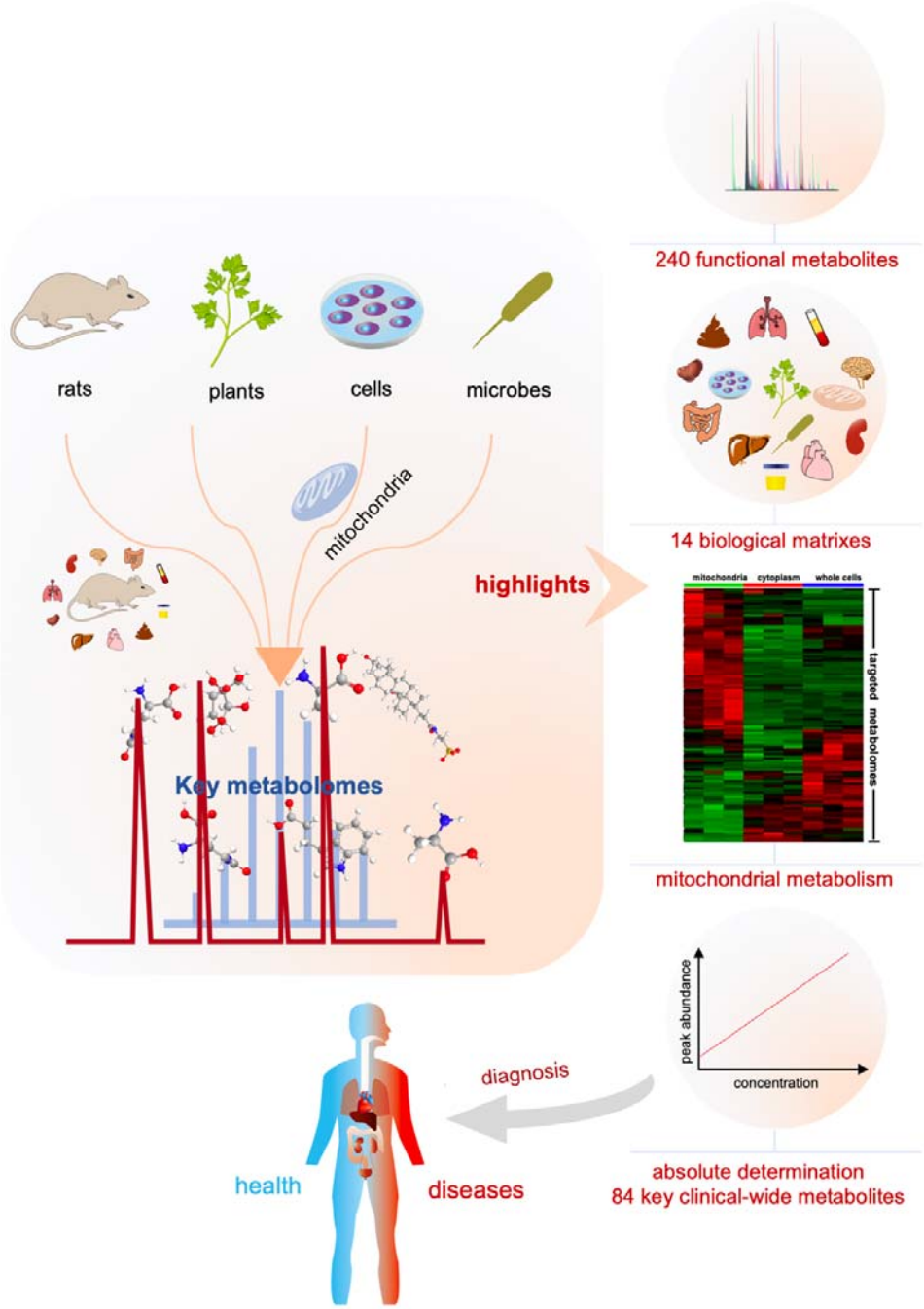
240 functional metabolites
rats
plants
cells
microbes
mitochondria
14 biological matrixes
highlights
mitochondria
cytoplasm
whole cells
targeted metabolomes
Key metabolomes
mitochondrial metabolism
peak abundance
concentration
diagnosis
health
diseases
absolute determination
84 key clinical-wide metabolites

Figure 8

Table S1. LC-TQ dynamic-MRM parameters of metabolomes

Metabolites	Transition	CE	Polarity	Retention time (min)	Column	Quantification
Salicylic acid	139.0 /121.0	13	Positive	10.28	T3	AQ
L-Lactic acid	89.0 /45.2	9	Negative	1.51	T3	AQ
Pyruvate	87.0 /43.2	5	Negative	1.143	T3	AQ
Malic acid	133.0 /115.0	9	Negative	1.31	T3	AQ
Fumaric acid	115.0 /71.1	5	Negative	1.52	T3	AQ
Succinic acid	117.0 /73.1	9	Negative	2.31	T3	AQ
N-Acetylglutamic acid	188.05/128.0	9	Negative	1.88	T3	AQ
2-Ketobutyric acid	101.0 /57.2	5	Negative	1.82	T3	AQ
Creatine	132.1 /90.1	13	Positive	1.02	T3	AQ
L-Arginine	175.2 /70.2	29	Positive	0.96	T3	AQ
Indole-3-acetic acid	176.1 /130.1	17	Positive	10.23	T3	AQ
Acetylcoenzyme A	810.14/303.2	33	Positive	11.47	T3	RQ
Ethyl 4-hydroxybenzoate	167.2 /139.1	9	Positive	11.76	T3	AQ
Indole-3-propionic acid	190.2 /130.1	21	Positive	11.52	T3	AQ
Hippuric acid	180.2 /105.1	13	Positive	7.094	T3	AQ
Cinnamoylglycine	204.1 /160.1	9	Negative	9.51	T3	AQ
Chenodeoxycholic acid	391.3 /373.5	37	Negative	12.91	T3	AQ

Cholesterol	387.3 /105.0	25	Positive	12.74	T3	AQ
4-Hydroxybenzoic acid	137.02 /93.1	9	Negative	6.652	T3	AQ
2-Hydroxycinnamic acid	163.0 /119.1	9	Negative	9.693	T3	AQ
L-Valine	118.1 /72.2	9	Positive	1.54	T3	AQ
L-Leucine	132.2 /86.2	17	Positive	2.527	T3	AQ
Maleic acid	115.0 /71.1	9	Negative	1.62	T3	AQ
Eupatorin	345.3 /284.1	33	Positive	12.58	T3	AQ
Fmoc-cit-OH	398.4 /179.2	25	Positive	11.99	T3	AQ
Fmoc-cys(tbu)-OH	400.2 /179.0	29	Positive	13.41	T3	AQ
3-Isobutyl-1-methylxanthine	223.1 /167.0	21	Positive	9.3	T3	AQ
N-ethylmaleimide	126.1 /80.0	21	Positive	5.932	T3	AQ
Dimethyl 3,4-furandicarboxylate	185.2 /153.1	9	Positive	9.959	T3	AQ
Dimethyl(S)-malate	163.1 /103.1	5	Positive	5.56	T3	AQ
Lipoic acid	205.3 /171.0	5	Negative	12.25	T3	AQ
8-hydroxy-2-deoxyguanosine	284.1 /168.0	13	Positive	4.82	T3	AQ
5-Hydroxy-L-tryptophan	221.2 /204.1	9	Positive	4.34	T3	AQ
Itaconic acid	129.0 /85.1	5	Negative	4.65	T3	AQ
Indoxyl sulfate	212.0 /80.1	25	Negative	6.87	T3	AQ
Azelaic acid	187.1 /125.0	13	Negative	9.86	T3	AQ

Dexamethasone	393.2 /373.2	5	Positive	12.02	T3	AQ
Sebacic acid	201.1 /183.1	13	Negative	11.16	T3	AQ
N-Acetyl-L-cysteine	164.2 /122.1	5	Positive	3.38	T3	AQ
N-Acetyl-L-tryptophan	245.1 /203.1	13	Negative	9.04	T3	AQ
N-Acetyl-L-methionine	192.3 /144.1	9	Positive	6.197	T3	AQ
5-aminosalicylic acid	154.2 /136.0	13	Positive	1.54	T3	AQ
5-Methylcytidine	258.3 /126.2	17	Positive	1.605	T3	AQ
3-Phenylpropionylglycine	208.2 /105.1	21	Positive	9.19	T3	AQ
Uracil	113.1 /70.1	17	Positive	1.51	T3	AQ
Citraconic acid	129.1 /85.2	9	Negative	2.97	T3	AQ
Methylmalonic acid	117.0 /73.2	9	Negative	2.743	T3	AQ
Uridine	243.1 /199.9	9	Negative	2.009	T3	AQ
Deoxycytidine	228.2 /112.2	5	Positive	1.541	T3	AQ
Thymine	127.1 /110.1	13	Positive	2.92	T3	AQ
2-Deoxyguanosine	268.1 /152.1	9	Positive	3.75	T3	AQ
Adenine	136.1 /119.0	25	Positive	1.47	T3	AQ
2'-Deoxyinosine	251.1 /134.9	21	Negative	4.27	T3	AQ
Hypoxanthine	137.0 /55.2	33	Positive	1.57	T3	AQ
P-Coumaric acid	163.0 /119.2	13	Negative	8.48	T3	AQ
Rosmarinic acid	359.1 /161.0	13	Negative	9.87	T3	AQ

Tryptamine	161.1 /144.1	9	Positive	6.61	T3	AQ
Serotonin	177.2 /160.2	13	Positive	4.339	T3	AQ
L-Kynurenine	209.09/192.1	5	Positive	4.89	T3	AQ
L-Methionine	150.2 /104.2	9	Positive	1.482	T3	AQ
S-(5'-Adenosyl)-L-homo cysteine	385.1/136.1	17	Positive	2.72	T3	AQ
Vanillic acid	167.0 /152.0	13	Negative	7.306	T3	AQ
3-Hydroxybenzoic acid	137.0 /93.0	9	Negative	6.9	T3	AQ
Biotin	245.3 /227.1	13	Positive	7.57	T3	AQ
Quercetin	303.1 /153.0	37	Positive	11.39	T3	AQ
Rotenone	395.4 /213.1	25	Positive	13.34	T3	AQ
Daidzein	255.1 /91.0	45	Positive	10.91	T3	AQ
Cyanocobalamin	678.5/147.1	49	Positive	6.85	T3	AQ
Lipoamide	206.4 /189.1	5	Positive	10.75	T3	AQ
6-Aminocaproic acid	132.1 /114.2	9	Positive	1.642	T3	AQ
Isonicotinic acid	124.1 /80.2	21	Positive	1.07	T3	AQ
Nicotinic acid	124.1 /80.2	21	Positive	1.51	T3	AQ
Protocatechualdehyde	139.0 /93.1	13	Positive	6.68	T3	AQ
Benzenesulfonic acid	157.0 /80.1	33	Negative	3.51	T3	AQ
Thiazolyl Blue	335.1 /77.0	25	Positive	11.997	T3	AQ
Caffeic acid	179.0 /135.1	17	Negative	7.47	T3	AQ
Pyridoxal	168.1 /150.0	13	Positive	1.7	T3	AQ
dUMP	307.03/194.7	13	Negative	1.6	T3	AQ
Cytidine monophosphate	324.2 /112.2	9	Positive	1.178	T3	AQ

2'-Deoxycytidine 5'-monophosphate	308.1 /112.1	5	Positive	1.48	T3	AQ
Adenosine 5'-monophosphate	348.1 /136.0	25	Positive	1.51	T3	AQ
Inosine-5'-monophosphate	349.1 /136.9	9	Positive	1.57	T3	AQ
Guanosine 5'-monophosphate	364.1 /151.9	13	Positive	1.68	T3	AQ
Phenylpyruvate	163.0 /91.2	9	Negative	7.684	T3	AQ
Rifampin	823.4 /791.2	17	Positive	12.48	T3	AQ
1,2-diacyl-sn-glycero-3-phospho-l-serine	792.58/607.7	21	Positive	5.79	Amide	RQ
1,2-Dioctadecanoyl-sn-glycero-3-phospho-rac-(1-glycerol)	777.560/283.4	45	Negative	2.62	Amide	RQ
Dioleoyl-sn-glycero-3-phosphoethanolamine	744.560/603.6	25	Positive	3.35	Amide	RQ
L-α-phosphatidylcholine	758.6/184	37	Positive	3.81	Amide	RQ
Phosphoenolpyruvic acid	168.99/150.9	5	Positive	9.34	Amide	RQ
CoQ10	863.7/197	33	Positive	0.88	Amide	RQ
5-Methylcytosine	126.1 /109.0	21	Positive	4.99	Amide	RQ
D-Pantothenic acid	220.120/90.2	13	Positive	2.26	Amide	RQ
Shikimic acid	173/93	9	Negative	4.4	Amide	RQ
1,2-Dipalmitoyl-sn-glycero-3-phosphocholine	734.570/184.1	33	Positive	3.36	Amide	RQ
Sphingomyelin	703.7/184.1	25	Positive	4.51	Amide	RQ
FMOC-GLN(TMOB)-O	549.6 /181.1	13	Positive	12.98	T3	RQ

H						
Trimethoprim	291.2 /230.1	25	Positive	7.26	T3	RQ
Heptadecanoic acid	269.250/251	21	Negative	13.97	T3	RQ
Butylated hydroxytoluene	219.2/203.1	29	Negative	14.44	T3	RQ
L-Norleucine	132.1 /86.1	9	Positive	2.68	T3	RQ
N-Acetylglutamine	189.2 /130.2	9	Positive	1.6	T3	RQ
Gluconic acid	195.05/129.2	13	Negative	0.94	T3	RQ
Oxaloacetic acid	131/87.1	5	Negative	1.13	T3	RQ
Tryptophan	205.1/188.1	9	Positive	5.71	T3	RQ
Cytosine	112.1 /95.1	17	Positive	1.54	T3	RQ
2'-Deoxyuridine	229.2 /113.0	12	Positive	2.863	T3	RQ
Adenosine	268.3 /136.2	17	Positive	3.35	T3	RQ
2-Deoxyadenosine	252.1 /136.0	13	Positive	3.71	T3	RQ
2'-Deoxyguanosine 5'-monophosphate	348/152.1	13	Positive	1.6	T3	RQ
p-Hydroxyphenylpyruvate	181.05/135.1	9	Positive	8.01	T3	RQ
p-Hydroxyphenylpropionic acid	165.05/121.2	9	Negative	7.96	T3	RQ
4-Hydroxyphenylacetic acid	151.04/107.1	9	Negative	6.89	T3	RQ
3-Indoleacrylic acid	188.07/170	13	Positive	10.84	T3	RQ
2-Methylhippuric acid	194.08/119.1	9	Positive	7.7	T3	RQ
Syringic acid	199.06/140.1	13	Positive	7.37	T3	RQ
Pyrogallol	127.04/109.1	13	Positive	3.2	T3	RQ

Phenylpropionic acid	149.06/105.1	5	Negative	11.4	T3	RQ
2-hydroxy-2-phenylpropanoic acid	165.05/121	9	Negative	8.3	T3	RQ
Indolepyruvic acid	204.07/158.1	13	Positive	11.05	T3	RQ
3-Hydroxyphenylpropionic acid	165.05/121	9	Negative	8.44	T3	RQ
Trans-Cinnamic acid	147.04/103	9	Negative	11.53	T3	RQ
Taurocholic acid	514.3/107.1	49	Negative	11.66	T3	RQ
Glycocholic acid	464.3/74.1	45	Negative	12.08	T3	RQ
Lithocholic acid	375.3/375.3	0	Negative	14.15	T3	RQ
Taurochenodeoxycholic acid	498.3 /124.0	50	Negative	12.16	T3	RQ
Deoxycholic acid	391.3 /345.2	37	Negative	13.38	T3	RQ
Taurodeoxycholic acid	498.3/123.9	50	Negative	12.25	T3	RQ
Tauroursodeoxycholic acid	498.3/123.9	50	Negative	11.66	T3	RQ
L-Phenylalanine	166.2 /120.1	13	Positive	4.67	T3	RQ
Isoleucine	132.2 /86.2	9	Positive	2.699	T3	RQ
Dopamine	154.2 /137.1	9	Positive	1.71	T3	RQ
Thiamine	266.1 /122.1	21	Positive	0.93	T3	RQ
Oxidized glutathione	613.2/354.9	21	Positive	2.04	T3	RQ
Glutathione	308.1 /178.9	9	Positive	1.59	T3	RQ

Beta-Sitosterol	415.4/119.2	29	Positive	13.08	T3	RQ
L-Carnitine	162.1 /103	17	Positive	1.1	T3	RQ
Normetanephrine	184.1/166	5	Positive	1.55	T3	RQ
Palmitoyl-l-carnitine	400.3/85.1	33	Positive	12.871	T3	RQ
Sphinganine	302.3/284.2	13	Positive	12.9	T3	RQ
Flavin adenine dinucleotide	784.150/436.9	29	Negative	6.23	T3	RQ
Uridine 5'-monophosphate	325.1 /97.0	9	Positive	1.13	T3	RQ
Acetylcholine	147.1 /87.1	13	Positive	1.19	T3	RQ
Dephospho-CoA	688.2/261.1	25	Positive	5.99	T3	RQ
Aminobutyric acid	104.1 /87.2	9	Positive	0.933	T3	RQ
2-Aminoimidazole	84.1 /42.2	28	Positive	1.033	T3	RQ
Allantoin	157.030/114.1	9	Negative	0.99	T3	RQ
1-Naphthylacetamide	186.230/141.1	21	Positive	10.85	T3	RQ
2,4-Diaminobutyric acid	119.1/101.2	5	Positive	0.828	T3	RQ
3-Guanidinopropionic acid	132.14/72.2	17	Positive	1.24	T3	RQ
D-Glucose 6-phosphate	259.020/97.1	17	Negative	0.89	T3	RQ
2-Ketoglutaric acid	145/101.1	5	Negative	1.483	T3	RQ
Cis-Aconitic acid	173.0 /111.1	5	Negative	1.9	T3	RQ
L-Aspartic acid	134.1/74.2	13	Positive	1.05	T3	RQ
L-Glutamic acid	148.1 /130.1	5	Positive	2.06	T3	RQ
L-Citrulline	176.2 /70.2	25	Positive	0.94	T3	RQ

N-Acetylornithine	175.2 /115.2	9	Positive	0.97	T3	RQ
L-Proline	116.1 /70.2	17	Positive	0.999	T3	RQ
Creatinine	114.07/86.1	9	Positive	1	T3	RQ
Putrescine	89.1 /72.2	5	Positive	0.76	T3	RQ
Sarcosine	90.1 /44.0	13	Positive	0.9	T3	RQ
Trans-4-Hydroxy-L-proline	132.1 /86.2	13	Positive	0.907	T3	RQ
Glyoxylic acid	72.99/45.2	5	Negative	0.9	T3	RQ
Betaine	118.2 /59.2	17	Positive	0.95	T3	RQ
Betaine aldehyde	102.2/58.3(59.2)+	20	Positive	0.9	T3	RQ
5-Aminolevulinic acid	132.1 /114.1	5	Positive	0.96	T3	RQ
L-Cystathionine	223.3 /88.1	29	Positive	0.88	T3	RQ
L-Threonine	120.1 /74.2	9	Positive	0.919	T3	RQ
L-Homoserine	120.1 /74.1	9	Positive	0.91	T3	RQ
Cytidine	244.2 /112.1	9	Positive	1.25	T3	RQ
Glycine	76.040/30.2	17	Positive	0.892	T3	RQ
Trimethylamine N-oxide	76.2 /58.2	21	Positive	0.915	T3	RQ
Glycochenodeoxycholic acid	448.3/386.1	37	Negative	12.64	T3	RQ
Cholic acid	407.3 /343.1	37	Negative	12.64	T3	RQ
Taurine	126.2/108.1	9	Positive	0.89	T3	RQ
Choline	105.1/61.2	17	Positive	0.874	T3	RQ
L-Carnosine	227.2 /210.2	9	Positive	0.93	T3	RQ
L-Cysteic acid	170.170/124.1	13	Positive	0.885	T3	RQ
L-Homocysteine	136.05/90.1	9	Positive	1.11	T3	RQ

Alanine	90.1 /44.3	17	Positive	0.9	T3	RQ
Glucosamine	180.1/162.1	5	Positive	0.85	T3	RQ
Glycolic acid	75.0 /47.2	9	Negative	1.08	T3	RQ
L-Ascorbic acid	177.0/95.1	9	Positive	1.435	T3	RQ
L-Lysine	147.2 /130.2	9	Positive	0.8	T3	RQ
Cysteamine	78.04/61.0	21	Positive	0.778	T3	RQ
Hypotaurine	110.03/92.1	5	Positive	0.78	T3	RQ
Agmatine	131.1 /72.2	17	Positive	0.88	T3	RQ
Inosine	269.09/137.1	29	Positive	3.25	T3	RQ
Histamine	112.1 /95.1	13	Positive	0.996	T3	RQ
L-Histidine	156.2 /110.1	13	Positive	0.84	T3	RQ
Ursodeoxycholic acid	391.280/373.3	33	Negative	12.69	T3	RQ
Beta-Glycerophosphate	171/79	45	Negative	0.93	T3	RQ
D-Tartaric acid	149.01/86.9	13	Negative	1.02	T3	RQ
Roxithromycin	837.5 /158.0	33	Positive	11.8	T3	RQ
Hexanoylcarnitine	260.1 /85.1	21	Positive	8.69	T3	RQ
Glucose	179.05/89	5	Negative	0.94	T3	RQ
2-Phospho-D-glyceric acid	184.98/78.9	29	Negative	1.2	T3	RQ
DHAP	168.9/96.9	9	Negative	0.95	T3	RQ
D-Glyceraldehyde 3-phosphate	168.99/97.2	9	Negative	0.99	T3	RQ
Citrate	191.1 /111.0	9	Negativ	1.655	T3	RQ

			e			
Succinyl coenzyme A	868.14/361.2	41	Positive	5.39	T3	RQ
Guanidineacetic acid	118.1 /72.1	9	Positive	0.95	T3	RQ
Spermidine	146.2 /72.2	17	Positive	0.71	T3	RQ
Malonic acid	103/59.2	9	Negativ e	1.36	T3	RQ
Glycodeoxycholic acid	450/414.2	13	Positive	12.74	T3	RQ
L-Histidinol	142.1 /124.1	9	Positive	1	T3	RQ
Pyridoxal 5'-phosphate	248.2 /150.0	17	Positive	1.63	T3	RQ
D-Fructose	179.1 /89.1	5	Negativ e	1.13	T3	RQ
Acetylcarnitine	204.2 /85.1	17	Positive	1.54	T3	RQ
Adenylosuccinic acid	464.1 /251.9	21	Positive	4.3	T3	RQ
NADH	664.1/407.8	33	Negativ e	4.12	T3	RQ
Oxalic acid	89/45.2	5	negativ e	0.91	T3	RQ
L-Asparagine	133.06/74.2	17	Positive	0.95	T3	RQ
Isocitric acid	191.02/111.1	13	Negativ e	1.17	T3	RQ
Dehydrocholic acid	403.25/385.2	9	Positive	12.4	T3	RQ
Taurolithocholic acid	484.31/466.5	9	Positive	13.35	T3	RQ
Taurohyodeoxycholic acid	500.31/464.4	13	Positive	11.79	T3	RQ
Caproic acid	117.09/73.2	9	Positive	0.75	T3	RQ
5-Dodecenoic acid	199.17/55.3	29	Positive	13.94	T3	RQ
3-Methylindole	132.08/117.1	25	Positive	12.96	T3	RQ
Ethylmethylacetic acid	103.08/73	5	Positive	0.96	T3	RQ
Arachidonic acid	305.25/79.1	49	Positive	14.24	T3	RQ

8,11,14-Eicosatrienoic acid	307.27/67.2	45	Positive	13.72	T3	RQ
Docosahexaenoic acid	327.23/283.3	9	Negative	15.15	T3	RQ
Melatonin	233.13/174.1	17	Positive	9.63	T3	RQ
Phenyllactic acid	165.05/147.1	9	Negative	8.44	T3	RQ
Pelargonic acid	159.14/43.3	13	Positive	13.4	T3	RQ
Decanoic acid	173.16/131.9	5	Positive	1.01	T3	RQ
Pentadecanoic acid	243.23/43.3	33	Positive	13.57	T3	RQ
Stearic acid	285.28/43.3	41	Positive	12.72	T3	RQ
Salicyluric acid	196.06/121.1	13	Positive	8.28	T3	RQ
Aminoadipic acid	162.08/98.1	13	Positive	1.07	T3	RQ
Norvaline	118.09/72.2	5	Positive	1.45	T3	RQ
3-Indoleacetonitrile	157.08/130.1	13	Positive	11.84	T3	RQ
Citramalic acid	147.03/87.1	13	Negative	2.21	T3	RQ
Pyroglutamic acid	130.05/84.1	13	Positive	1.78	T3	RQ
Glutaric acid	131.03/87.2	9	Negative	3.78	T3	RQ
Pipecolic acid	130.09/84.2	17	Positive	1.34	T3	RQ
L-Glutamine	147.08/130.1	5	Positive	0.88	T3	RQ
L-Ornithine	133.1/70.2	21	Positive	0.78	T3	RQ

AQ: Absolute Quantification; RQ: Relative Quantification

Table S2. Absolute determination of 84 key metabolites with calibration-curve

Metabolites	Linear range (ng/mL)	Calibration curve	R^2
Salicylic acid	2.5-1000	Y=2624.2X-4610.3	0.9998

Vanillic acid	2.5-1000	Y=2163.5X-10209.8	0.9998
Nicotinic acid	2.5-500	Y=47649.3X+192890	0.9997
Indole-3-propionic acid	2.5-500	Y=22900.9X+46815.8	0.9994
dUMP	12.5-1000	Y=955.7X-5855	0.9994
N-Acetylglutamic acid	2.5-1000	Y=1594.3X-4996.2	0.9991
Cinnamoylglycine	2.5-1000	Y=1725.5X+8798.5	0.9989
Benzenesulfonic acid	2.5-1000	Y=5340.4X+38032.9	0.9989
4-Hydroxybenzoic acid	2.5-1000	Y=1543X+9454.9	0.9988
3-Isobutyl-1-methylxanthine	2.5-250	Y=114641.8X+40652.2	0.9986
5-aminosalicylic acid	2.5-250	Y=73980.1X+157966.2	0.9986
Cyanocobalamin	2.5-1000	Y=8441.8X-95729.5	0.9985
Fumaric acid	2.5-1000	Y=596.2X+6360	0.9985
L-Kynurenine	2.5-1000	Y=18094.3X+97616.3	0.9984
Creatine	1.56-100	Y=54009.2X+144085.6	0.9984
P-Coumaric acid	2.5-1000	Y=2371.3X+28667.1	0.9982
N-Acetyl-L-tryptophan	2.5-1000	Y=2626.1X+18657.1	0.9981
Biotin	2.5-1000	Y=15839.5X+4783.6	0.9979
2-Hydroxycinnamic acid	2.5-1000	Y=1995.3X+23969.8	0.9975
Citraconic acid	10-1250	Y=1281.4X+19737.9	0.9975
Indoxyl sulfate	2.5-1000	Y=3994.7X+48714.7	0.9971
Lipoic acid	0.5-50	Y=9109.7X-11507.9	0.9967
Hippuric acid	5-500	Y=42888.8X+158271.3	0.9966
Chenodeoxycholic acid	62.5-1000	Y=4.2X-354.4	0.9965
2-Deoxyguanosine	2.5-1000	Y=26263X+651590.1	0.9963
Caffeic acid	2.5-500	Y=6884.7X+65740.9	0.9963
N-Acetyl-L-cysteine	2.5-500	Y=9459X-105383.1	0.9962
Cholesterol	0.5-50	Y=11407.8X+10664.3	0.9962
Rotenone	0.5-50	Y=31916X-13227.1	0.9959
Thymine	50-1000	Y=4804.1X+147480.3	0.9956
2'-Deoxyinosine	10-1250	Y=4086.1X+133624.3	0.9954
Cytidine monophosphate	2.5-1000	Y=11123.9X-158399.7	0.9951
Fmoc-cys(tbu)-OH	2.5-1000	Y=3137.4X-63556.6	0.995
Maleic acid	2.5-1000	Y=3884.6X+87802.4	0.9948
2'-Deoxycytidine 5'-monophosphate	2.5-1000	Y=8828.8X-233907.4	0.9947
Isonicotinic acid	2.5-500	Y=119179.9X+1848509.5	0.9947
Phenylpyruvate	10-1250	Y=568.5X-6634.7	0.9945
Fmoc-cit-OH	0.5-50	Y=325329.9X-143312	0.9944
3-Phenylpropionylglycine	5-500	Y=52539.4X+256602.1	0.9942
Rosmarinic acid	5-2000	Y=5588.7X+97664.4	0.9934
Methylmalonic acid	10-1250	Y=381.7X+17855.8	0.9931
N-Acetyl-L-methionine	2.5-1000	Y=7069.9X+128333.7	0.993
Dexamethasone	2.5-1000	Y=6594.6X+77157.6	0.9929
Protocatechualdehyde	2.5-1000	Y=6305.3X+142590.6	0.9929

3-Hydroxybenzoic acid	2.5-1000	Y=3881.4X+92292.5	0.9927
Serotonin	2.5-1000	Y=13867.7X+134201.9	0.9924
Adenine	2.5-250	Y=67087.2X+790897.1	0.9923
Itaconic acid	2.5-1000	Y=1532.1X+39902.8	0.9919
Dimethyl 3,4-furandicarboxylate	5-100	Y=327660.7X+1391516.5	0.9918
Ethyl 4-hydroxybenzoate	5-500	Y=35687.8X+372792.2	0.9918
Lipoamide	2.5-500	Y=12797X+169419.1	0.9913
5-Hydroxy-L-tryptophan	1.56-100	Y=24068.5X-92904.3	0.9912
Uridine	10-1250	Y=387.9X+18567.6	0.9912
8-hydroxy-2-deoxyguanosine	1.56-100	Y=14740X-56280.7	0.9907
Guanosine 5'-monophosphate	5-1000	Y=3726.7X-77860.9	0.9904
Adenosine 5'-monophosphate	2.5-1000	Y=10429.6X-322495.8	0.9903
Dimethyl(S)-malate	50-1000	Y=9642.1X+869793.2	0.99
L-Arginine	62.5-1000	Y=23681.3X-465300.4	0.99
Thiazolyl Blue	5-100	Y=117733.8X+471535.6	0.9888
5-Methylcytidine	2.5-500	Y=33341.3X+717161.8	0.9886
Uracil	5-500	Y=19981.8X+318592.6	0.9885
Rifampin	12.5-500	Y=87.8X-4012.2	0.9884
L-Methionine	2.5-1000	Y=3650.2X+114769.8	0.9883
Azelaic acid	2.5-1000	Y=3641.3X+136598.4	0.9882
Inosine-5'-monophosphate	2.5-500	Y=367.7X-6993.7	0.9878
Hypoxanthine	62.5-1000	Y=8037.4X+1575299.5	0.9871
Deoxycytidine	62.5-1000	Y=5231.1X+1573951.7	0.9866
N-ethylmaleimide	6250-80000	Y=162.6X+6115828.6	0.9865
6-Aminocaproic acid	2.5-500	Y=22150.4X+639770.1	0.9861
L-Valine	2.5-500	Y=32151.5X+521586.5	0.9845
Sebacic acid	5-500	Y=10385.5X+239366.4	0.9845
S-(5'-Adenosyl)-L-homocysteine	2.5-1000	Y=22127.8X+986168.4	0.9842
2-Ketobutyric acid	10-1250	Y=433.1X+29981.2	0.984
Eupatorin	0.5-50	Y=73582.7X+133465	0.9831
L-Leucine	2.5-1000	Y=41002.8X+812054.5	0.9829
Indole-3-acetic acid	1.56-100	Y=9099.2X-46024.3	0.9826
Pyridoxal	50-1000	Y=32722.9X+5582005	0.9824
Tryptamine	2.5-250	Y=72155.2X+1575771.6	0.9822
Daidzein	2.5-250	Y=21948.8X+367723.7	0.9819
Quercetin	12.5-1000	Y=810.5X-27194.9	0.9809
Malic acid	12.5-1000	Y=1693.7X-75073.9	0.9808
Succinic acid	6250-80000	y = 157.3X + 4139425.2	0.9795
Pyruvate	1250-80000	Y=18.9X+115530.6	0.9799
L-Lactic acid	1250-80000	Y=2.7X+119781.5	0.9600

Table S3. Concentration of representative 27 key metabolites in plasma, urine and a diverse tissues of rats (n=6)

Metabolites	Concentration (ng/mL)								
	Brain	Heart	Lung	Spleen	Kidney	Liver	Small intestine	Plasma	Urine
Rotenone	0.52±0.03	0.46±0.02	0.45±0.01	0.45±0.01	0.51±0.04	0.48±0.02	0.43±0.01	0.45±0.01	0.44±0.01
Lipoic acid	1.88±0.04	2.52±0.14	1.95±0.04	2.1±0.05	1.87±0.07	2.17±0.15	1.86±0.11	1.91±0.05	27.27±5.83
Eupatorin	3.2±0.3	541.1±538.39	626.87±620.42	3.9±0.42	9194.59±3281.69	2259.3±1010.62	3022.36±606.24	1317.92±589.75	60.6±36.14
5-Hydroxy-L-tryptophan	4.13±0.02	4.31±0.08	4.04±0.03	4.12±0.04	4.92±0.08	4.75±0.1	4.78±0.09	3.87±0.01	4.04±0.04
8-hydroxy-2-deoxyguanosine	24.84±19.75	41.84±34.12	78.11±72.75	236.3±73.71	7.28±1.28	356.99±45.33	7±1.08	5.8±0.32	47.27±9.76
dUMP	13.2±2.02	16.53±1.66	15.68±1.69	13.85±1.5	16.12±1.47	21.35±1.93	22.34±3.76	19.32±0.51	10696.48±2928.27
N-Acetylglutamic acid	13.87±2.63	324.95±82.88	7.68±0.7	7.79±0.68	486.43±102.85	288.67±81.64	16±4.3	11.3±0.61	617.35±486.15
Inosine-5'-monophosphate	21.6±0.58	21.06±0.19	21.56±0.4	21.36±0.37	20.41±0.13	20.51±0.14	21.43±0.43	26.26±0.34	24.04±2.38

			6						
Indole-3-acetic acid	31.7±3.38	139.92±117.65	52.29±2.34	1021.61±943.96	22.74±1.55	23.14±1.53	30.51±4.24	34.07±8.65	78.62±46.97
Adenosine 5'-monophosphate	32.18±0.15	44.08±2	52.7±2.03	37.65±0.81	47.9±2.51	38.25±1.45	33.64±0.64	123.55±8.1	582.92±143.7
Malic acid	45.04±0.11	46.91±0.13	45.92±0.11	46.3±0.19	45.76±0.19	45.99±0.19	147.36±101.65	44.58±0.26	55.01±3.33
2'-Deoxycytidine 5'-monophosphate	42.75±2.53	32.61±0.41	38.98±0.72	33.92±0.83	27.43±0.09	29.03±0.43	28.8±0.93	78.11±19.71	26.52±0.02
Cytidine monophosphate	37.33±3.75	28.95±4.77	25.92±1.12	25.02±0.92	42.22±2.04	43.14±2.35	20.56±0.42	62.53±6.02	181.63±54.53
4-Hydroxybenzoic acid	76±5.7	78.81±13.05	174.69±19.68	41.49±2.73	84.56±13.25	62.43±7.49	144.86±19.22	32.38±13.73	857.02±224.95
N-Acetyl-L-cysteine	37.96±7.55	644.03±115.07	17.6±1.18	29.68±6.99	13.05±0.2	74.97±26.86	37.81±4.98	12.13±0.32	11.3±0.09
Vanillic acid	96.28±4.3	804.15±25.	154.4±6.7	239.31±6.7	116.52±3.58	102.68±5.27	212.9±18.98	198.56±11.	34.89±10.87

	9	77		2				96	
Guanosine 5'-monophosphate	93.39±2.78	596.36±18.85	142.85±5.72	196.94±2.54	108.45±2.73	93.95±2.57	185.91±14.92	173.04±6.84	42.48±7.79
Cinnamoylglycine	112.2±10.15	225.28±17.49	238.61±26.38	234.87±7.96	74.65±7.83	36±1.88	173.11±29.4	304.92±28.21	29.02±23.39
Quercetin	128.4±8.51	44.96±1.06	44.44±1.76	173.67±6.85	45.33±1.05	36.88±1.37	325.05±72.54	104.27±5.69	50.08±6.27
L-Arginine	175.28±13	504.46±19.82	359.11±12.68	387.61±28.05	890.46±26.09	551.9±27.81	753.88±26.58	52.49±5.05	27.62±3.35
L-Kynurenine	179.04±2.83	243.77±8.9	185.54±8.98	156.34±3.77	156.21±6.63	268.27±8.76	1266±711.29	372.66±204.8	1353.53±432.66
Dexamethasone	245.88±13.56	187.32±13.2	397.53±20.03	636.78±44.93	171.75±10.15	148.27±14.69	219.14±35.62	52.71±26.64	3.87±14.3
Cholesterol	246.48±18.86	141.6±18.48	123.73±13.58	206.33±16.52	329.03±40.04	264.85±28.64	177.72±45.05	9.5±1.67	15.73±3.7
Ethyl 4-hydroxybenzoate	259.24±2	555.57±28.	551.43±25	1048.87±30	1469.62±37.	649.06±25.24	580.59±127.4	1078.29±54	57.45±14.2

	3.79	89	.09	.15	4		5	.71	
Chenodeoxycholic acid	378.82±78.25	606.96±196.07	931.17±358.64	260.93±50.92	489.91±90.74	12102.13±1412.05	14128.96±5535.57	277.26±51.01	90.44±2.21
Creatine	722.5±15.54	687.38±12.01	455.58±28.5	679.24±21.13	442.86±89.19	733.66±20.62	140.5±62.14	1.28±0.86	0.13±1.52
Cyanocobalamin	768.09±56.44	1396.83±221.68	601.39±137.56	465.06±20.08	495.35±34.73	663.14±122.32	606.12±27.64	51.71±5.28	33.62±10.46